SUPERSATURATION, DROPLET SPECTRA, AND TURBULENT MIXING IN CLOUDS

H. Gerber
Naval Research Laboratory, Washington, DC 20375-5000

I. Introduction

Much effort has recently gone into explaining the observed broad precoalescence size distribution of droplets in clouds and fogs, because this differs from the results of condensational growth calculations which lead to much narrower distributions. The correct explanation of this difference is important, since the observed broadening has a strong influence on the optics of the clouds, as well as on their colloidal stability. Existing explanations, which have yet to be proved definitive, have generally dealt with the interaction of turbulence with the cloud, such as in entrainment and mixing (Telford et al., 1984; Jonas and Mason, 1982; Baker et al., 1980; Clark and Hall, 1979; and many others). Most have dealt with the "favored-droplet hypothesis", which states that due to the statistical nature of turbulence some "favored" droplets experience a lifetime in the clouds which is more conducive to condensational growth (or evaporation) than other droplets, and hence cause the broadening (e.g., Cooper, 1989).

A good example of droplet size-distribution broadening was observed on flight 17 (25 July) of the NRL tethered balloon during the 1987 FIRE San Nicolas Island IFO. On this date a stratocumulus cloud cover formed rapidly from clear sky conditions. The balloon was aloft at the time, and was able to penetrate the Sc clouds 7 min. after their formation. These virgin clouds, which could not include the complexity of upwind evolution, contained significant numbers of 32.5 μ diameter droplets (the largest size bin of the CSASP particle spectrometer). Such large droplets cannot easily be explained by a standard updraft argument. Instead, observed RH and wind shear in the vicinity of these clouds suggested a formation mechanism which included Kelvin-Helmholtz induced mixing of a nearly saturated layer. These observations motivated us to take another look at the interaction between cloud microphysics and turbulent mixing. We used the findings of Broadwell and Breidenthal (1982) who conducted laboratory and theoretical studies of mixing in shear flow, and those of Baker et al. (1984) who applied the earlier work to mixing in cloud. Rather than looking at the 25 July case at SNI, we chose instead to look in detail at earlier fog observations made at SUNY (6 Oct., 1982) which also indicated that shear-induced mixing was taking place, and which had a better collection of microphysical measurements including more precise supersaturation measurements (see Gerber, 1980 for description of technique) and detailed vertical profiles of meteorological parameters; see Fig. 1.

In this study we address the following questions:

1. Does B-B (Broadwell-Breidenthal) mixing, or gradient diffusion control droplet evolution in shear situations involving nearly saturated air?
2. Can B-B mixing account for the observed large transient supersaturations which can last as long as tens of seconds?
3. Can B-B mixing account for strong droplet broadening and the appearance of the largest droplets?

II. Broadwell-Breidenthal Mixing

B-B mixing describes a mixing process different from the usual approach in which turbulent mixing occurs via gradient diffusion. The latter is only reasonably successful when the scale of the turbulence is small in comparison to

the distance across which the diffusing quantity is changing significantly. Broadwell and Breidenthal (1982) clearly demonstrated in laboratory measurements that gradient diffusion between two species in shear flow does not hold, but is instead governed by another mechanism consisting essentially of a two stage mixing process: For most of the lifetime of a decaying eddy containing two species, the identity of the species remains largely intact. Only as the Kolmogorov microscale is reached do the two species rapidly mix with each other by molecular diffusion.

We first apply B-B mixing to an eddy with properties estimated from the 6 Oct. fog case. The eddy had a characteristic dimension L = 6.9m, it consisted of two saturated parcels with a difference in temperature of 3°C (which is the maximum temperature difference observed over the height of the micromet tower), and it contained droplets with a size distribution given by curve 0715 in Fig. 1 and measured at about RH = 100%. We derive an expression similar to the classical equation

$$S(t) = Q_1 \int dh - Q_2 \int dw \qquad (1)$$

giving the time evolution of supersaturation S(t) in terms of the mass balance of total water in an ascending cloud parcel (e.g., see Squires, 1952). Instead of the excess (supersaturated) vapor released by the change in height dh of the parcel, we include the release of excess vapor by the B-B mixing of the saturated parcels. Under isobaric conditions, and under the assumption that the rate of release of excess moisture is proportional to the rate of formation of interfacial area between the two saturated parcels in the eddy we find

$$S(t) = \left[\left(\frac{x}{x_s K} - 1\right)\left(1 - \frac{t_k}{\tau_L}\right)^{3/2}\left(1 - \frac{t}{\tau_L}\right)^{-3/2}\right] - \left[\frac{1}{\rho_a x_s K}\int \sum_r 4\pi r N(r) C\left(S(t) - \frac{A}{r} + \frac{B}{r^3}\right) dt\right] \qquad (2)$$

$$K = \frac{L^2 M_o \Delta w}{R \bar{T}^2 C_p} + 1$$

where x = vapor mixing ratio of mixed eddy, x_s = saturation mixing ratio of mixed eddy, w = liquid water mixing ratio, N(r) = particle density at radius r, C = rate constant, t_k = time to reach Kalmogorov turbulence scale, τ_L = time for complete homogenization, and other symbols have the usual meaning.

The predictions of (2) are illustrated in Fig. 2. The curve labeled 0715 shows a rapid release of excess moisture at around 35 sec of the calculation, with a maximum value of S near the maximum S = 0.43% that can be achieved by mixing two saturated parcels with a 3-°C temperature difference, and with a decrease of S from the maximum corresponding to the takeup by growing droplets and lasting tens of seconds. Curve 0719 corresponds to the use of the distribution labeled 0719 in Fig. 1 as the initial condition (initial LWC = 0.09 g/m^3); and the curve for X10 uses the 0719 distribution with 10 times the LWC value. We can conclude from Fig. 2 that (a) the B-B mixing mechanism causes the formation of transient supersaturations in the fog, (b) the release of excess vapor is faster than the time scale of droplet response, and (c) the time constant of the decay of the transient S is approximately proportional to the integral radius of the droplets as is evident from the second term of (2).

These conclusions are supported by the observations in the 6 Oct. fog. Mixing was clearly shear induced as indicated by the stable temperature profile, gradient diffusion could not have caused the observed supersaturation transients because of the magnitude of the temperature gradient, and the observed transients were of a magnitude consistent with the maximum temperature differences observed with height.

III. Broadening of Droplet Size Distribution

An important consequence of B-B mixing as illustrated in Fig. 2 is that the release of excess vapor appears to be essentially independent of the droplet content, and thus can be treated separately from the conversion of the vapor to liquid, which depends approximately on the integral radius. It is thus possible to use the droplet growth equation

$$r\frac{dr}{dt} = C\left(S - \frac{A}{r} + \frac{B}{r^3}\right) \tag{3}$$

with an average S parameterized in terms of the integral radius, if the maximum value of S(t) is measured or estimated.

To fully exploit this possibility, the integral form of (3) was rewritten to give a set of analytical expressions

$$r \simeq f\left(r_o, S, t, r_d\right) \quad \text{for} \quad \begin{cases} r_d > 10^{-6}\text{cm} \\ r_o > r_d \\ S > -1 \\ t > 0 \\ \text{particle type} \end{cases} \tag{4}$$

which give one-equation solutions to the time dependence of r, given S (r_o = initial radius, r_d = dry nucleus radius). This approach greatly speeds up the calculations, because (3) is implicit in r and usually requires numerical integration, and is difficult to use for small droplets. Equation (4) is mathematically well behaved, and it gives the proper transitions between activated droplets and haze particles; see Fig. 4. Equation (4) should be useful in improving the coupling between microphysics and dynamic models.

A model was developed to evaluate the effects of B-B mixing on droplet broadening. The approach, as in Nichols (1987), was to combine the effects of stochastic turbulent diffusion with explicit microphysical calculations. However, in the present case only droplet growth by diffusion is considered. Furthermore, this model, rather than being driven by models of turbulent diffusion, is driven by the observed statistics of S and eddy size (see Fig. 3). Highlights of the model include: The Monte-Carlo approach is used to randomly mix eddies in a Lagrangian framework. The mixing process includes contributions from mixing eddies proportional to their volume, and conserves particle concentration, liquid water volume, and total nuclei volume. Calculations are done in N(r) space using (4), and timescales are estimated from Eulerian observations of eddy frequency and the droplet integral radius.

Some initial runs of the model are shown in Figs. 5 and 6. Using the measured cumulative probability of S and L shown in Fig. 3 with the 0715 size distribution to initialize the model, results in the droplet spectrum for t = 15 min shown in Fig. 5. On the average droplets have evaporated to smaller sizes

in this case. This is consistent with the slightly subsaturated conditions reflected by the means in Fig. 3. The statistics in Fig. 3 were collected 1.5-m above a grassy surface in post sunrise fog where some warming of the surface was taking place. The second example in Fig. 6, which illustrates the flexibility of this model, shows a double-peaked distribution with significant broadening and maximum droplet sizes close to the ones observed in the 6 Oct. fog. For this case the S distribution in Fig. 3 was biased by S = + .001, the time scale of the excess S decay was set at a constant 20 s, and 80% of the final eddies making up the distribution in Fig. 6 correspond to t = 3 min while the rest is for t = 15 min. Other runs of the model (not shown), using S decay coupled to the integral radius as suggested by B-B mixing, gave significantly broadened size distributions, but none with peaks in the size distribution exceeding about 10 μm diameter even for t = 60 min.

IV. Conclusions

The observations in the 6 Oct. fog and the initial results of the stochastic condensational growth model suggest the following conclusions on the importance of Broadwell-Breidenthal mixing in fogs and clouds:

(a) B-B mixing of nearly saturated parcels at different temperature causes large transient supersaturations as observed in the 6 Oct. and other fogs.

(b) These transient supersaturations and turbulent mixing cause droplet spectral broadening governed by the "favored droplet hypothesis".

(c) The effect of B-B mixing on droplet broadening is approximately proportional to the temperature difference of nearly saturated mixing parcels and inversely proportional to the integral droplet radius, thus hazes and clouds of low LWC with strong temperature gradients will see the largest effects.

(d) B-B mixing could not explain the observation of 30-μm diameter droplets in the 6 Oct. fog. The rapid increase of droplet size observed 1.5-m above the surface is partially explained by the downward mixing of this fog which formed 20 min earlier aloft. It is proposed that B-B mixing contributes primarily to the mid-size peak (about 5 μm diameter) often found in these fogs, and that the large droplet peak is due to very large supersaturations generated by another mechanism found higher up in the fog.

Baker, M.B., R.G. Corbin and J. Latham, 1980: The influence of entrainment on the evolution of cloud droplet spectra: I. A model of inhomogeneous mixing. Quart. J. Roy. Met. Soc., 106, 581-598.

Baker, M.B., R.E. Breidenthal, T.W. Choularton and J. Latham, 1984: The effects of turbulent mixing in clouds. J. Atmos. Sci., 41, 299-304.

Broadwell, J.E., and R.E. Breidenthal, 1982: A simple model of mixing and chemical reaction in a turbulent shear layer. J. Fluid Mech., 125, 397-410.

Clark, T.L., and W.D. Hall, 1979: A numerical experiment on stochastic condensation theory. J. Atmos. Sci., 36, 470-483.

Cooper, W.A., 1989: Effects of variable droplet growth histories on droplet size distributions. Part I: Theory. J. Atmos. Sci., in print.

Gerber, H.E., 1980: A saturation hygrometer for the measurement of relative humidity between 95% and 105%. J. Appl. Meteor., 19, 1196-1208.

Jonas, P.R., and B.J. Mason, 1982: Entrainment and the droplet spectrum in cumulus clouds. Quart. J. Roy. Met. Soc., 108, 857-869.

Nicholls, S., 1987: A model of drizzle growth in warm, turbulent, stratiform clouds. Quart. J. Roy. Met. Soc., 113, 1141-1170.

Squires, P., 1952: The growth of cloud drops by condensation. Aust. J. Sci. Res. A, 5, 59-86.

Telford, J.W., T.S. Keck and S.K. Chai, 1984: Entrainment at cloud tops and the droplet spectra. J. Atmos. Sci., 41, 3170-3179.

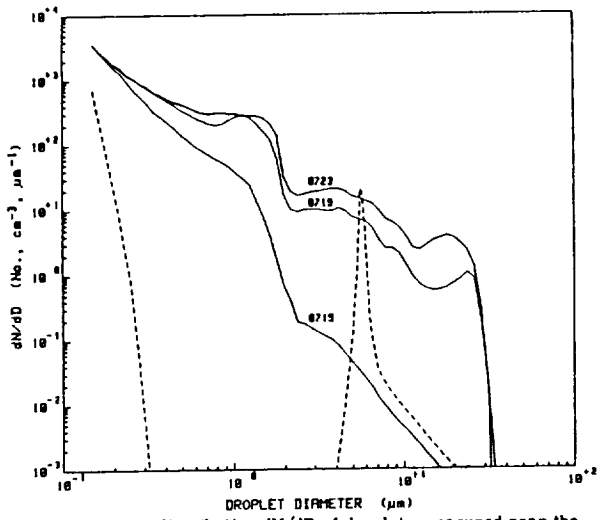

Fig. 1 - Size distribution dN/dD of droplets measured near the surface at indicated times in the fog on 6 Oct. Dashed curve results from classical condensational growth calculations with S = 0.001 for 5 min. with 0715 as the initial distribution.

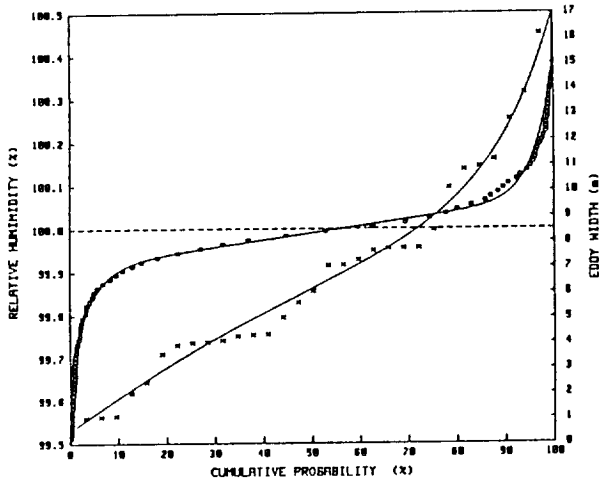

Fig. 3 - Cumulative probability distributions of supersaturation (o) and eddy width (x) measured near the surface during the 6 Oct. fog.

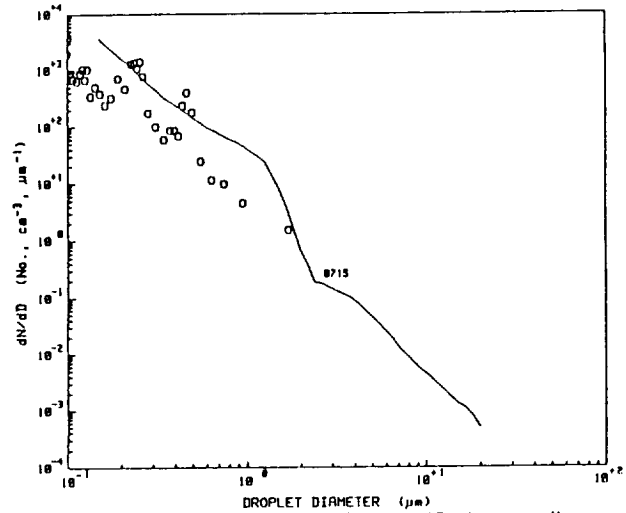

Fig. 5 - Predicted evolution of dN/dD after 15 min. according to the stochastic condensational growth model using the statistics in Fig. 3 and the 0715 distribution for initialization.

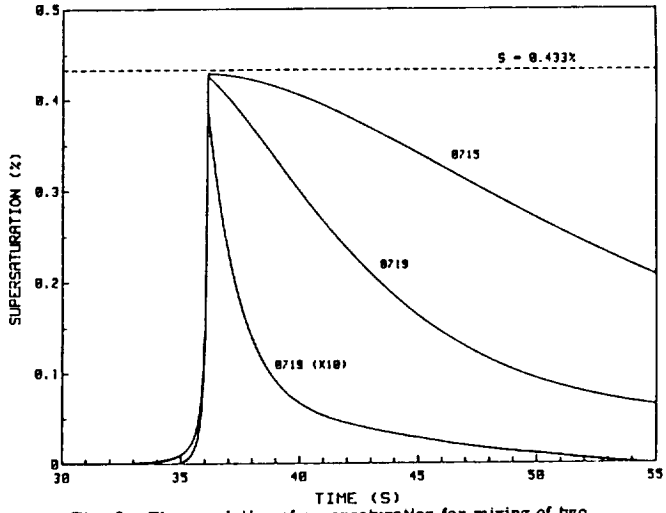

Fig. 2 - Time evolution of supersaturation for mixing of two saturated parcels with a temperature difference of 3 °C and different initial droplet size distributions, according to the Broadwell-Breidenthal mixing mechanism.

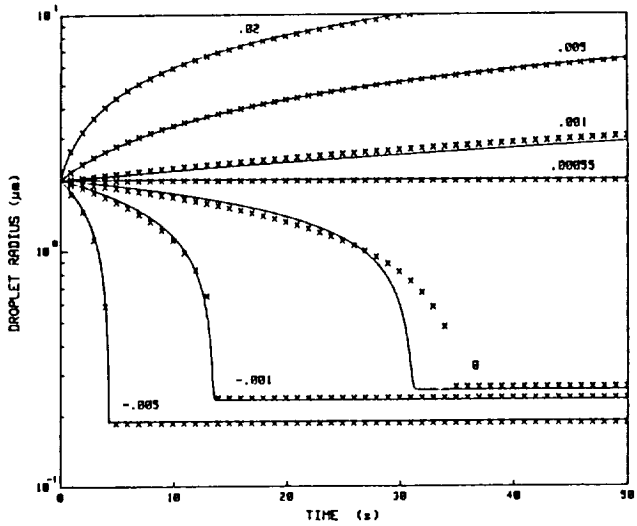

Fig. 4 - Comparison of the growth rate of a 2-um droplet formed on an urban nucleus calculated with the exact growth equation (3) and with the approximate analytical expressions (4;x) as a function of the indicated supersaturations.

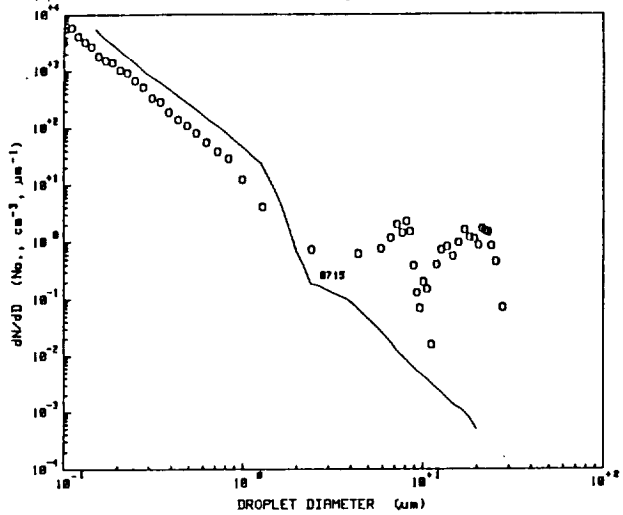

Fig. 6 - Same as Fig. 5, except that supersaturation statistics in Fig. 3 were biased by S = + 0.001, and parcels with different time histories were averaged.